LASERS

PACS numbers: 42.55.Lt; 42.60.Mi; 42.65.Sf
DOI: 10.1070/QE2001v031n01ABEH001885

Study of the dynamics of propagation of CO_2 laser pulses in a chain of nonlinear absorbing and amplifying media

K N Makarov, D D Malyuta, S G Nishchuk, V C Roerich, Yu A Satov, Yu B Smakovskii, A E Stepanov, S V Khomenko

Abstract. **In the system consisting of a master oscillator, a three-pass telescopic amplifier, and saturable absorbing cells, CO_2 laser pulses with an energy of 100 J and duration variable from 15 to 80 ns were obtained. A theoretical model for the calculation of interaction of CO_2 laser radiation with resonance absorbing and amplifying media was developed. The system consisting of an absorber saturated at the leading edge of the pulse and an amplifier working in the deep-saturation mode was shown to provide a considerable increase in the gain and pulse compression.**

Keywords: *nonlinear dynamics, saturable absorber.*

1. Introduction

The generation of CO_2 laser pulses with prescribed spatial, time, and energy characteristics is a necessary condition for the efficient use of such lasers in a variety of applications. In particular, to obtain the maximum number of multiply charged ions in ion beams in a laser plasma [1], one needs laser pulses that are much smaller in duration than a radiation spike in a free running mode.

At present, master oscillator-power amplifier systems are extensively used for controlling laser pulse duration. The main method of controlling the output pulse duration consists in tailoring the shape of a master oscillator (MO) pulse and subsequent amplification of this pulse in one or several amplifying stages. To form pulses in a MO, one can use an electrooptical shutter, an appropriate choice of parameters of a laser cavity, a laser mixture, and pumping conditions, and filters with saturable absorbers. In this work, we used the last two methods to form 15 – 80-ns pulses.

The basic physical processes governing the formation of time characteristics of a laser pulse in resonance amplifying, absorbing, and combined media are described in Refs [2 – 5] on the basis of a two-level model. In particular, the rate and the law of rise of the leading edge of a pulse being amplified were shown to be the main physical factors determining the duration and the shape of the output pulse. In these works, pulse shortening was obtained under the assumption that the MO pulse had the Gaussian shape. This pulse shape is difficult to obtain in practice. In most cases, MOs operating in the free running mode provide an exponential increase in the pulse intensity. The nonlinear character of amplification in these cases leads only to the shift of the pulse peak in time [3], without changes in the pulse duration and the law of rise of its leading edge.

This paper is devoted to the study of conditions of formation of CO_2 laser pulses upon their successive propagation through a nonlinear absorber and a CO_2 amplifier. An important specific feature of the study is the use of the absorption filter saturation at the leading edge of the pulse and a strongly saturated amplification mode. This allowed us to avoid considerable losses in absorbing filters and to shorten a pulse in an amplifier, simultaneously increasing the output power.

2. Experimental

The optical scheme of the setup is presented in Fig. 1. It includes a single-mode single-frequency MO *1*, which uses the hybrid scheme [6]; a three-pass power amplifier *14* with an off-axis Cassegrain telescope consisting of two mirrors *12* and *13*; absorbing cells *2* (AC1) and *11* (AC2), which are filled with an air – SF_6 mixture; a diffraction grating *3*; and a spatial filter containing two spherical mirrors *4* and *5* and an aperture *6*. The power amplifier was constructed on the basis of a module with an electron-beam-controlled electric discharge [7]. The chamber with an active amplifying medium was 15 cm × 15 cm × 100 cm in size.

The optical scheme of the three-pass amplifier was formed by plane mirrors *7 – 10*, which provided the first

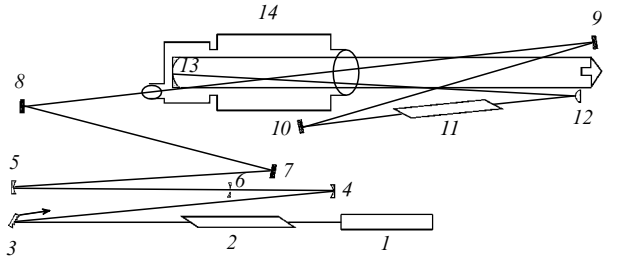

Figure 1. Optical scheme of the setup: (*1*) master oscillator; (*2, 11*) absorbing cells; (*3*) diffraction grating; (*4, 5*) confocal spherical mirrors; (*6*) aperture; (*7, 10*) plane mirrors; (*12*) convex spherical mirror; (*13*) focusing spherical mirror; (*14*) amplifier.

K N Makarov, D D Malyuta, S G Nishchuk, V K Rerikh, Yu A Satov, Yu B Smakovskii, A E Stepanov, S V Khomenko State Scientific Centre of Russian Federation – Troitsk Institute for Innovation and Thermonuclear Research, 142092 Troitsk, Moscow oblast, Russia

Received 12 September 2000
Kvantovaya Elektronika **31** (1) 23 – 29 (2001)
Translated by by A Kirkin

passage in the amplifier, and the off-axis confocal telescope *12, 13* with magnification $M = 6.6$, with the large mirror 150 mm in diameter. A diffraction grating *3* (100 lines/mm) provided optical coupling of the MO to the amplifying system at the $P(20)$ line of the 10-μm amplification band. Absorbing cells with an air – SF_6 mixture, which fulfilled the role of saturable filters for the $P(20)$ line, were used to form the time profile of a pulse being amplified. The problems of suppression of parasitic lasing and a backward pulse in the amplifying system are discussed in Refs [8, 9].

To study the radiation pulse shape, we used photon-drag detectors with the 0.7-ns resolution. The detector signals were recorded with a Lecroy 9450 digital two-channel oscilloscope with the 350-MHz amplification band and the 2.5-ns digitization step. The measurements of the rate of rise of the leading edge of a MO and amplified pulses are described in detail in Ref. [9]. The shape of MO pulses was typical of a CO_2 laser. It depended on the mixture composition and the cavity Q factor. For the 35 % effective reflectivity of cavity mirrors and the $CO_2 : N_2 : He = 4 : 1 : 5$ composition of a gas mixture, the pulse had the highest rate of rise of the leading edge (with the exponential factor $t_0 = 8 - 9$ ns) and the 74-ns FWHM at an energy of 250 mJ. The pulse energy was measured by standard calorimetric detectors. In all the experiments, the small-signal gain g_0 in the amplifying module was ~ 0.04 cm^{-1}.

3. Nonlinear characteristics of amplifying and absorbing media

In spite of a large number of works devoted to the study and application of saturable SF_6 cells in laser systems, systematic data on the effect of their parameters on the time characteristics of CO_2 laser pulses are unavailable in the literature. A satisfactory theoretical model for the description of SF_6 kinetics in a sufficiently wide range of parameters is also absent. In this paper, the optical characteristics of cells were determined by measuring the transmission of SF_6 cells in a wide range of pulse energies and intensities. The experimental data were extrapolated to the region of low intensities and were included, together with the characteristics of the pulse amplification process, in the calculation program.

Fig. 2 presents the dependences of the cell transmission on the intensity and energy of an input pulse for the cells 11 and 68 cm long filled with pure SF_6 and a mixture of SF_6 with air, which was used as a buffer gas for increasing the relaxation rate and changing the absorber saturation intensity. Using a series of measurements with cells of different length, we empirically determined the optimum absorber parameters that are matched to the length of the amplifier used in our experiments (curve *2* in Fig. 2). In particular, the optimum lengths of AC1 and AC2 were found to be 68 and 45 cm, respectively.

4. Results of formation of time and energy characteristics of a radiation pulse

The time and energy parameters of a laser pulse are formed in resonance media of an absorber and an amplifier. For the given energy and shape of the MO pulse and amplification length, parameters of the output laser pulse depend on many factors, which include geometric characteristics of the laser beam (the beam diameter during the first passage

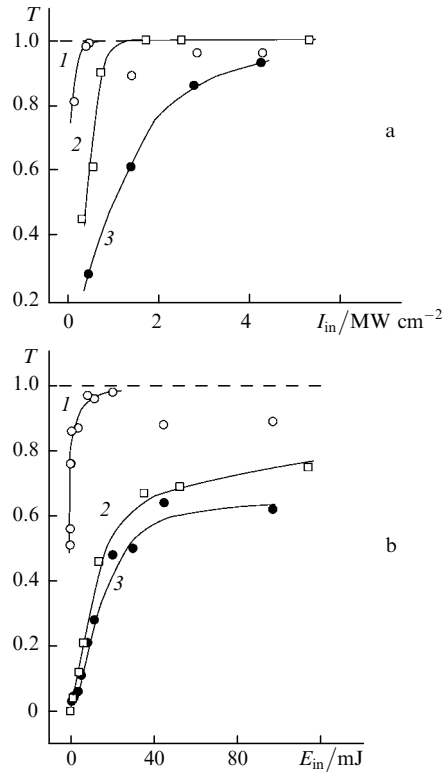

Figure 2. Dependences of the cell transmission on the input radiation intensity (a) and energy (b) for the cell 11 cm long with pure SF_6 at a pressure of 0.5 mbar (*1*), the cell 68 cm long with the mixture of SF_6 (0.08 mbar) with air (450 mbar) (*2*), and the cell 11 cm long with the mixture of SF_6 (0.5 mbar) with air (600 mbar) (*3*).

through the amplifier, the initial and final diameters during the second passage, the telescope magnification, etc.) in addition to the nonlinear properties of media.

Results of the preliminary study of the amplification scheme are described in Ref. [9]. It is shown there that in the case of a MO with a low-Q cavity, the leading edge with the rise time $t_0 = 13$ ns, and the use of only AC2 with pure SF_6 at a pressure of 0.5 mbar, the output pulse retains the duration (80 ns at half-maximum) and its peak is 60 ns ahead of the peak of the input pulse. In this case, an increase in the steepness of the output pulse was observed only at signal levels below 10^{-4} of the peak magnitude. The use of AC1 with a higher saturation intensity provided a considerable increase in the steepness of the input pulse, a noticeable shortening of the output pulse, and the aforementioned advance of the pulse peak.

Systematic measurements and adjustment of the scheme were performed using a MO cavity with a higher Q factor ($R_{eff} = 35$ %) and, therefore, a steeper time profile of the pulse intensity (see below Fig. 5, curve *1*). In these experiments, the lengths of AC1 and AC2 (68 and 45 cm) were fixed. The parameters of the optical scheme and the amplifier ($g_0 = 0.04$ cm^{-1}) were also unchanged. We measured the output radiation characteristics (pulse energy, half-width of a pulse and the duration of its leading edge) as functions of parameters of absorbing cells (pressure of working and buffer gases).

Fig. 3 presents the results of optimisation of AC1 in the absence of AC2. The data are obtained by averaging the results of three successive measurements. One can clearly see that there exists an optimum combination of partial pres-

sures of SF_6 and the buffer gas at which the maximum shortening of the output pulse was observed. Under these conditions, the decrease in the output energy with respect to its value for the system without an absorbing cell was found to be small, lower than 10 %, and the pulse power reached a maximum value (curve *2*).

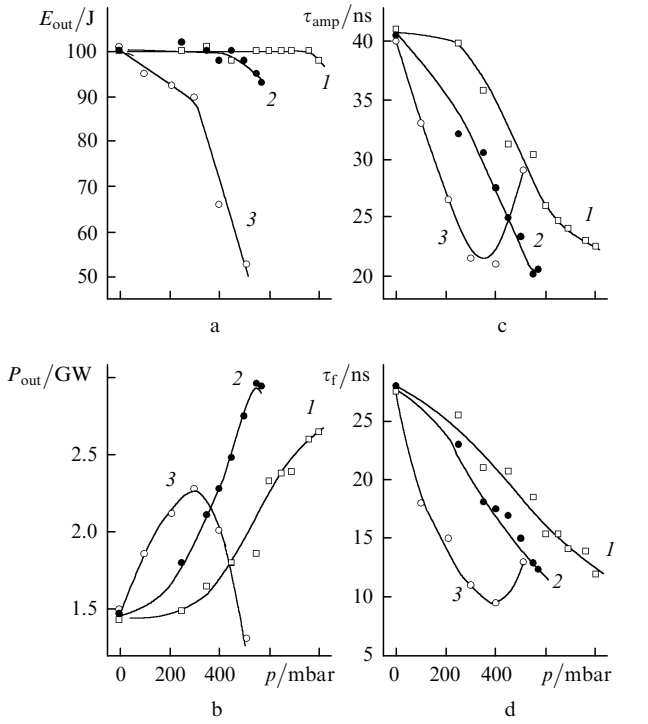

Figure 3. Dependences of the energy (a), power (b), FWHM (c), and the rise time of the leading edge (d) of the output pulse on the buffer gas pressure in AC1 68 cm long for an SF_6 pressure of 0.05 (*1*), 0.075 (*2*), and 0.2 mbar (*3*).

At large absorption coefficients (i.e., at a large partial pressure of SF_6) and an increased cell saturation intensity (buffer pressure), the pulse shortening was efficient (curves *3*), but the losses in the absorbing cell were substantial and were not compensated for in an amplifier of finite length. In the case of a cell with an insufficiently high optical density (low absorber pressures), an increase in pulse steepness was weak (curves *1*) and the pulse compression did not reach the maximum possible degree even at large buffer gas pressures, which corresponds to high saturation intensities of the absorbing medium.

Similar measurements were made for AC2 at fixed parameters of AC1. Fig. 4 presents the dependences of the output amplifier parameters on the buffer gas pressure in AC2 at the optimum SF_6 pressure. Typically, at a fixed absorber density (SF_6 pressure), a pulse is efficiently shortened, with the output energy being unchanged, with increasing buffer gas pressure up to a certain critical value. Above this value, the losses in the absorber become substantial and the deterioration of the output characteristics is observed.

Fig. 5 presents oscillograms of the MO pulses and the output pulses for different parameters of the system. In our experiments, we obtained pulse shortening down to 15 ns at half-maximum. This is the limiting value for the parameters realised for the elements of the optical scheme (the amplification length and the rise time of the MO pulse) and characteristics of absorbing filters.

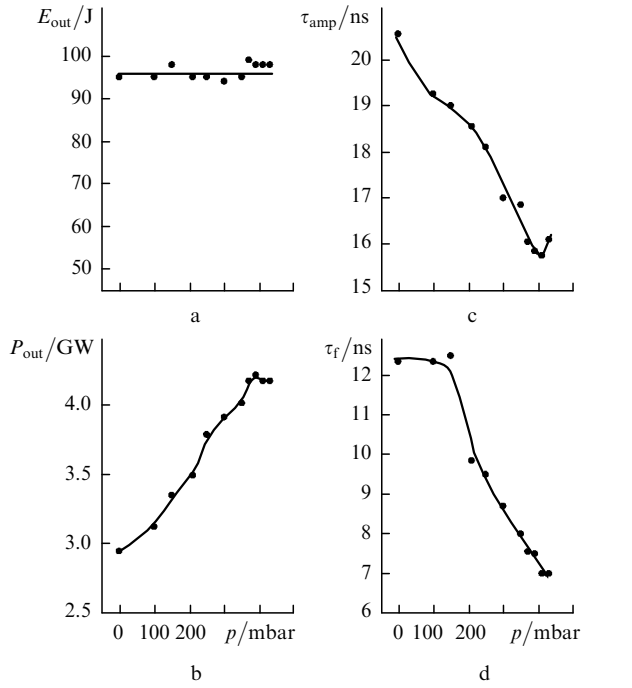

Figure 4. Dependences of the energy (a), power (b), FWHM (c), and the rise time of the leading edge (d) of the output pulse on the buffer gas pressure in AC2 45 cm long for an SF_6 pressure of 0.075 mbar. All parameters of AC1 are fixed and correspond to curve *2* in Fig. 3.

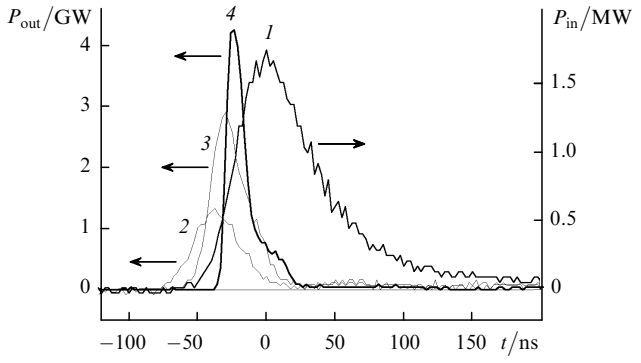

Figure 5. Oscillograms of MO radiation (*1*) and of the output pulses in the absence of cells (*2*), for the optimum parameters of AC1 in the absence of AC2 (*3*), and for the optimum parameters of both cells (*4*).

5. Theoretical model, calculation results, and their comparison with the experiment

The experimental conditions described in the paper correspond to the incoherent amplification mode, which substantially simplified the theoretical model. The model of vibrational kinetics used here is based on the harmonic-oscillator approximation [10–12]. The model of the CO_2 kinetics is based on the assumption that we have the equilibrium energy distribution over vibrational states in each of the three fundamental vibrational modes of a molecule, which is characterised by the corresponding temperature. To take into account two-dimensional effects during the

propagation of the MO pulse in the active medium of the amplifier, the computer program SHOLAS2D was developed. The geometry used in the calculation is shown in Fig. 6.

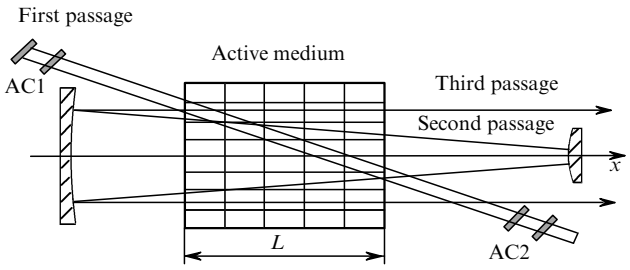

Figure 6. Geometry of the calculation in the SHOLAS2D program.

The active medium is assumed to have the cylindrical symmetry about the x axis. The pulse propagation was calculated on a rectangular uniform (x, r) grid. The number of calculation cells was typically 30-40 in the longitudinal direction and 20 – 30 in the radial direction. Because optical beams formed on different passages considerably differ in radial size, we used a separate grid for the first passage. This grid is not shown in Fig. 6 because of the difference in scales. The calculations were carried out under the assumption that radiation during the first passage travelled as a parallel beam and that the beam axis lay in the plane of the axial cross section of the active medium. The points of beam entrance and exit on the first passage were specified by the coordinates y_1 and y_2, respectively. Because the second and the third passages overlap, the saturation of the active medium depends on the sum of intensities. In each cell of the main volume of the active medium and the separate calculation grid of the first passage, we solved the system of equations of vibrational kinetics for CO_2 and N_2 molecules [10 – 14].

Because of the complexity of kinetic processes in the SF_6 molecule, the pulse propagation was calculated using the semi-empirical model based on the two-level approximation. A laser beam was assumed to have a plane wave front. The expression for the absorption coefficient was taken in the form $\alpha = \alpha_0/(1 + I/I_s)$, where α_0 is the small-signal absorption coefficient, I is the laser radiation intensity, and I_s is the saturation intensity. Thus, it was assumed in the model that the absorption coefficient corresponded to the instantaneous intensity, which is valid for the cells with a large pressure of the buffer gas. Because the dynamic range of measurements of the transmission of absorbing cells did not allow one to determine experimentally the coefficient α_0, the latter was treated as a fitting parameter, as well as I_s. The radial intensity distribution in the input beam was assumed to be Gaussian, with the width corresponding to the experimental value. The pulse shape also corresponded to the experimental one.

To calculate the transmission, we solved the equation of radiation transfer along the cell $dI(r, x)/dx = -\alpha I(r, x)$. The output radiation intensity $I_{out}(r, t)$ obtained in this way was integrated over the radius and time, which provided the calculation of transmission for the given total input energy.

5.1 Model calculations of gain in the one-dimensional geometry

The amplification of a parallel beam was calculated for studying the variation of the shape of the MO pulse during its propagation in the amplifying medium under different conditions in a saturable absorber. The aim of this series of calculations was to find the effect of the main parameters of an 'ideal' absorbing cell, namely, the initial optical thickness and the saturation intensity, on the amplified pulse duration.

Figs 7 and 8 illustrate some results of the numerical calculation of the laser pulse shape and the pulse rise time $R(t) = [(1/I)(dI/dt)]^{-1}$ during the pulse propagation in the amplifying medium up to the gain $g_0L = 18$ for different parameters of the absorbing filter. The energy density of the pulse $\mathscr{E}_0 = 110$ mJ cm^{-2} and its shape ($t_0 = 10$ ns) at the input of the scheme corresponded to the experimental conditions and provided amplification saturation ($\mathscr{E}_0/\mathscr{E}_s \sim 0.3$). One can determine from Figs 7 and 8 the shift of the amplified pulse relative to the MO pulse.

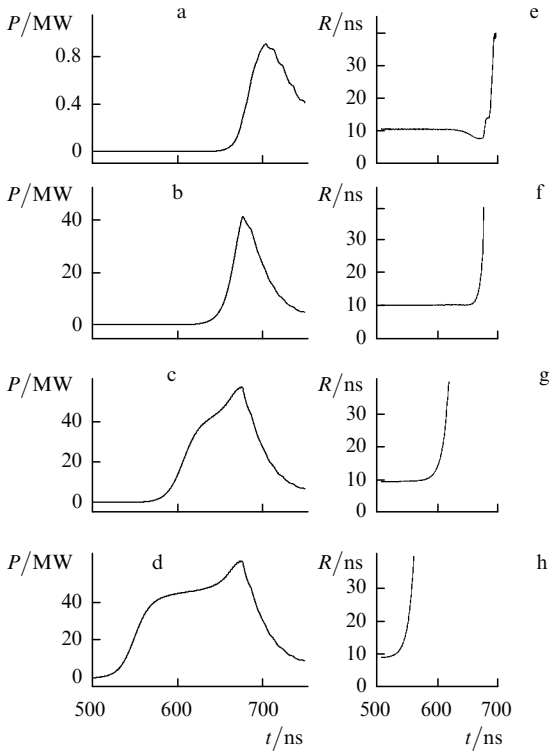

Figure 7. Calculated pulse shapes (on the left) and the rise time R of the leading edge of the pulse (on the right) for the absorption coefficient $\alpha_0 = 1.31$ and $I_s = 0.14$ MW cm^{-2} for the amplification length $L = 0$ (a, e), 150 (b, f), 300 (c, g), and 450 cm (d, h).

As follows from the calculations, in the absence of an absorber, the form of the exponential leading edge of the pulse remains unchanged, and a certain decrease in its duration at the initial amplification stage is caused by amplification saturation and a sharper decay of the trailing edge. In this case, the shift of the leading edge of a pulse in the forward direction is considerable, and this hinders an efficient power amplification. The stationary power is achieved at g_0L as small as 5 – 6. Further on, the pulse is lengthened because of the formation of a double-peaked structure. The formation of this structure is caused by a rather slow decay of the trailing edge of the input pulse and, partially, by the relaxation of the lower laser level, which is substantial for CO_2 at atmospheric pressure in the case of pulses longer than 10 – 20 ns (intramode relaxation).

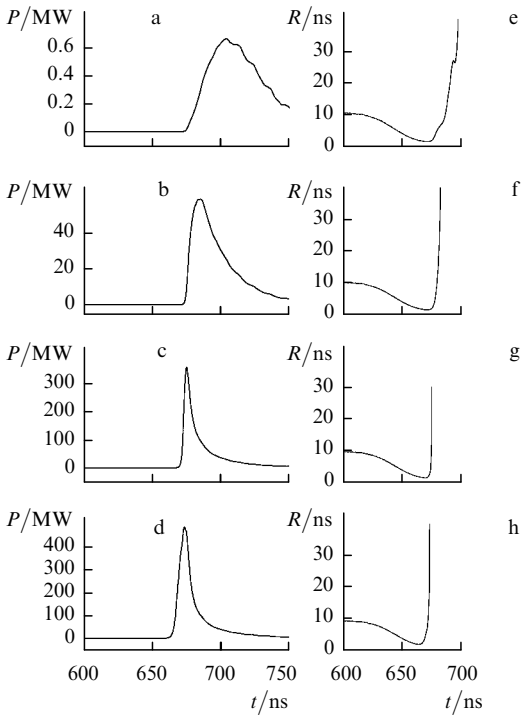

Figure 8. Calculated pulse shape (on the left) and rise time R of the leading edge of the pulse (on the right) for $\alpha_0 = 21.4$ and $I_s = 0.02$ MW cm^{-2} for the amplification length $L = 0$ (a, e), 150 (b, f), 300 (c, g), and 450 cm (d, h).

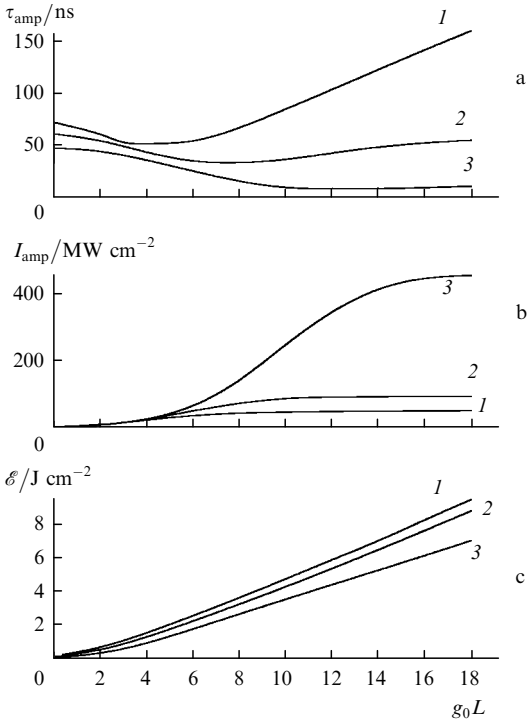

Figure 9. Calculated dependences of the duration (a), intensity (b), and energy density (c) of the amplified pulse on the gain for $\alpha_0 = 0.43$, $I_s = 0.01$ MW cm^{-2} (*1*), $\alpha_0 = 1.31$, $I_s = 0.14$ MW cm^{-2} (*2*), and $\alpha_0 = 21.4$, $I_s = 0.02$ MW cm^{-2} (*3*) for $t_0 = 10$ ns.

The use of an absorbing cell with a noticeable absorption coefficient that is saturated at the leading edge of the pulse ($\alpha_0 = 1.31, I_s = 0.14$ MW cm^{-2}, Fig. 7) enables one to increase the steepness of the leading edge of the pulse that enters the amplifier approximately 30 ns before the peak of the input pulse (Fig. 7e). This provides pulse shortening down to 45 ns at the gain $g_0 x \simeq 6$ (Fig. 7a) after the corresponding shift of the pulse peak towards the leading edge. Upon further amplification, the pulse 'runs' ahead where the leading edge has the previous exponential form and it begins to lengthen because of the formation of a complex double-peaked shape (Fig. 7d). A considerable increase in the efficiency of power amplification of a pulse and its simultaneous compression are obtained in a cell with a high optical density and a relatively low saturation intensity ($\alpha_0 = 21.4$, $I_s = 0.02$ MW cm^{-2}, Fig. 8). A substantial increase in the pulse steepness after the passage through this filter (Fig. 8e) leads to pulse compression to about 7 ns after saturated amplification on a 300-cm path (Fig. 8c).

The dependences of the pulse duration at half-maximum, the intensity, and the energy density at the amplifier output on the gain $g_0 L$ are presented in Fig. 9 for different parameters of an absorbing cell. Note that the pulse power in any case reaches a stationary value after the passage of the amplification length that corresponds to the minimum duration of the output radiation, i.e., the pulse is amplified in power only at the stage of its efficient shortening. The pulse energy linearly increases with gain $g_0 L$ after reaching sufficient saturation.

The model enabled us to calculate the optimum parameters of the optical scheme (the amplification length and the absorber saturation intensity) for different coefficients of small-signal absorption in a cell with a fixed length ($l = 68$ cm). The results of this calculation are shown in Fig. 10 (curves *5, 6*). The same figure presents characteristics of the radiation pulse at the output of the cell (curves *1, 2*) and after its amplification on the optimum length (curves *3, 4*). The MO pulse had an exponential leading edge with the rise time $t_0 = 10$ ns and the peak intensity $I_0 = 1.1$ MW cm^{-2}. One can see from the calculations, that the losses in the nonlinear absorber for the maximum α_0 considered here do not exceed 40 %, whereas the power at the amplifier output linearly increases with increasing optical thickness, and the pulse is efficiently shortened. The model calculations confirm the experimental data on the optimum absorption coefficients for a weak signal and the saturation intensity for the given amplification length (Fig. 3).

Note that as the optical cell thickness $\alpha_0 l$ increases from 0.5 to 20, the optimum gain $g_0 L$ increases from 4 to 12 and the required saturation intensity I_s/I_0 decreases from 0.5 to 0.02. In the case of low optical densities of the absorber (and, correspondingly, small optimum amplification lengths), compression is weak and pulse shortening after the passage through the nonlinear absorber is comparable to the shortening after the passage through the amplifier. An important practical conclusion is that the power of the pulse being amplified can increase with increasing amplification length only when the optical density of the absorber at the input is increased (Fig. 10, curves *4* and *6*) and its saturation intensity simultaneously decreases (Fig. 10, curve *5*).

Similar calculations were made for the input pulse with the rise time $t_0 = 5$ ns and the same total energy. The maximum intensity of this MO pulse increase up to 800 MW cm^{-2} compared to 450 MW cm^{-2} for the pulse with $t_0 = 10$ ns, and the limiting pulse duration reaches 4.3 ns instead of 7 ns under the same conditions in the absorbing cell and for the same amplification lengths. It was experimentally shown in [7] that the shortening of the leading

edge of a MO pulse leads to a substantial increase in the efficiency of pulse compression in an amplifier.

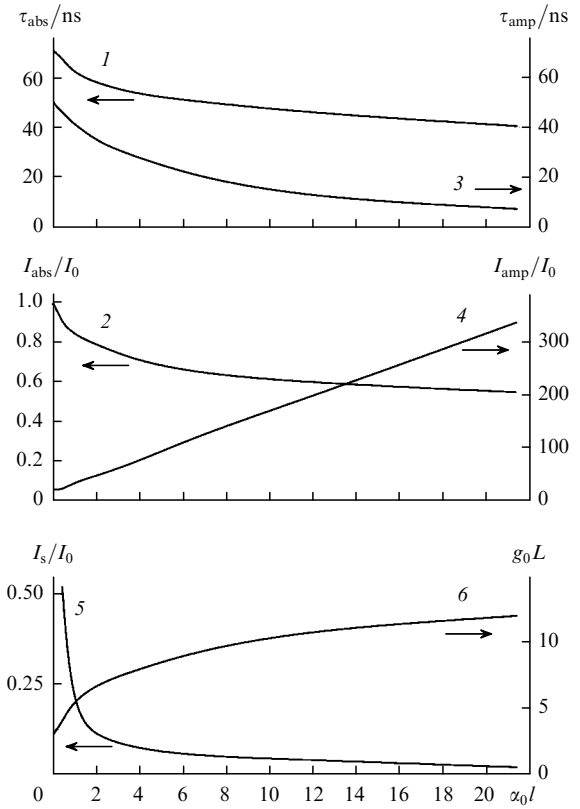

Figure 10. Calculated durations and intensities of the pulse at the output of the absorbing cell τ_{abs} (*1*) and I_{abs} (*2*) and after its amplification on the optimum length τ_{amp} (*3*) and I_{amp} (*4*) and the optimum saturation intensity I_s (*5*) and gain g_0L (*6*) versus $\alpha_0 l$ in the cell with the length $l = 68$ cm.

The pulse shortening after the passage through a nonlinear absorber was maximum for $I_s/I_0 = 0.7 - 0.8$ in all the interval of α_0 used in the calculations, which corresponds to the conclusions of Refs [2, 4] for the similar model of an absorbing medium. However, we did not study this regime here because of large losses in the cell. For instance, the shortening of the input pulse ($t_0 = 5$ ns) in the absorbing cell from 71 to 14 ns was accompanied by a decrease in its power by a factor of 300.

5.2 Results of the calculation of pulse amplification in a real amplifier

Calculations of the amplification in the real geometry of a three-pass amplifier showed that the main properties found in model one-dimensional calculations remain valid. In the experiments, a pulse makes its first passage in the amplifier near the anode surface, where the gain is noticeably higher than in the most part of the active medium. Because of this, the pump power that we set for the first passage was somewhat higher than for the next passages. The calculated time dependence of the gain agrees well with the experiment.

The oscillograms of the MO pulse obtained in the experiments had a noticeable noise level both at the leading and trailing edges. To describe the output pulse shape correctly, the shape of the input pulse should be sufficiently smooth down to very low intensities. Because the MO pulse was obtained in the free running mode, its leading edge was assumed to rise exponentially. To exclude false spikes in the output pulse that are caused by MO pulse modulation due to electrical noise, the leading edge of the pulse was approximated by an exponential with the rise time determined from the smooth part of an oscillogram. The calculation started with the intensity equal to $\sim 10^{-6}$ of the peak value.

Fig. 11 presents the results of the calculation of amplification for the real MO pulse processed in this way. The cell parameters were chosen in accordance with the results of the measurement of its transmission for different input energies. One can easily see that both the duration of the amplified pulse and the time shift of its peak agree well with the experimental data presented in Fig. 5.

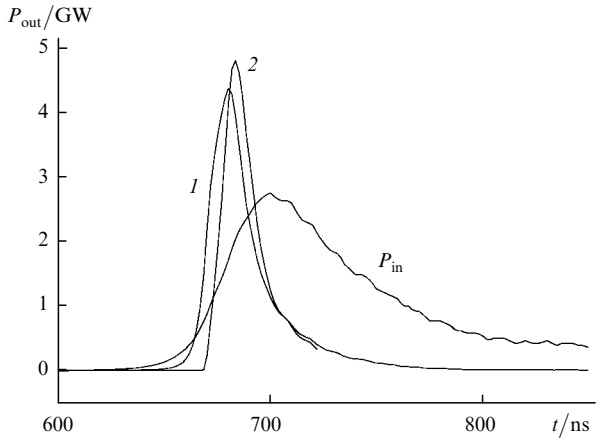

Figure 11. Shape of the input MO pulse $P_{in}(t)$ (scaled) and the calculated output pulses in the case of one (*1*) and two (*2*) cells.

6. Conclusions

The use of a combination of a nonlinear saturable absorber and an amplifier working in the deep-saturation mode is an efficient way of forming time characteristics of a laser pulse. This method provided a simple variation of the output laser pulse duration from 80 to 14 ns for the fixed shape of the MO pulse, with the output energy of ~ 100 J. Our theoretical model well describes the pulse propagation in absorbing and amplifying media and makes possible quantitative interpretation of the experimental results.

To obtain efficient amplification and compression of a CO_2 laser pulse, it suffices to form a portion of the leading edge of the MO pulse with a higher rate of the intensity rise and provide an appropriate amplification length. It is not required to reach the maximum shortening of the input pulse directly behind an absorbing cell; moreover, this regime is inefficient because of large losses. It is important to match parameters of a nonlinear filter (the small-signal absorption coefficient and the saturation intensity) to the length and geometry of the laser beam amplification that provide the desired saturation level. The pulse power increases with increasing amplification length only until a certain critical length, which depends on the steepness of the leading edge of the input pulse. As the amplification length is increased further, the pulse begins broaden again, and its power ceases to increase.

Acknowledgements. The authors thank A P Napartovich for his useful advises and critical remarks. This work was supported by the Russian Ministry of Science and the International Science and Technology Centre, project No. 495.

References

1. Baranov V Ya, Makarov K N, Roerich V C, et al. *Laser Particle Beams* **14** 347 (1996)
2. Kryukov P G, Letokhov V S *Usp. Fiz. Nauk* **99** 169 (1969)
3. Basov N G, Ambartsumyan R V, Zuev V S, Kryukov P G, Letokhov V S *Zh. Eksp. Teor. Fiz.* **50** 23 (1966)
4. Basov N G, Kryukov P G, Letokhov V S, Matveets Yu A *Zh. Eksp. Teor. Fiz.* **56** 1546 (1969)
5. Khartsiev V E, Stasel'ko D I, Ovchinnikov V M *Zh. Eksp. Teor. Fiz.* **52** 1457 (1967)
6. Makarov K N, Rerikh V K, Skatov Yu A, et al. *Kvantovaya Elektron.* **30** 305 (2000) [*Quantum. Electron.* **30** 305 (2000)]
7. Baranov V Yu, Bevov R K, Satov Yu A, et al. *Appl. Opt.* **15** 1373 (1976)
8. Khomenko S V, Makarov K N, Roerich V C, Satov Yu A, Stepanov A E *Preprint No. 0045-A* (Moscow: TRINITI, 1998)
9. Makarov K N, Nishchuk S G, Rerikh V K, Satov Yu A, et al. *Preprint No. 0069-A* (Moscow: TRINITI, 2000)
10. Manes K R, Seguin H J J. *Appl. Phys.* **43** 5073 (1972)
11. Smith K., Thompson R M *Computer Modeling of Gas Lasers* (New York: Plemum, 1978)
12. Witteman W J *The CO_2 Laser* (Berlin: Springer-Verlag, 1987)
13. Velikhov E P, Baranov V Yu, Letokhov V S, et al. *Impul'snye CO_2 Lazery i Ikh Primenenie dlya Razdeleniya Izotopov* (Pulsed CO_2 Lasers and Their Application for Isotope Separation) (Moscow: Nauka, 1983)
14. Baranov V Yu, Borisov V M, Napartovich A P, et al. *Preprint No. 2398* (Moscow, Institute of Atomic Energy, 1974)